

## Intraparticle Ripening Creating Hierarchically Porous Ti-MOF Single Crystals for Deep Oxidative Desulfurization

Shen Yu,<sup>‡ab</sup> Zhan Liu,<sup>‡abc</sup> Jia-Min Lyu,<sup>a</sup> Chun-Mu Guo,<sup>a</sup> Yi-Long Wang,<sup>d</sup> Zhi-Yi Hu,<sup>ac</sup> Yu Li<sup>a</sup>,  
Ming-Hui Sun,<sup>a</sup> Li-Hua Chen,<sup>\*a</sup> and Bao-Lian Su<sup>\*ac</sup>

\* To whom correspondence should be addressed: Li-Hua Chen ([chenlihua@whut.edu.cn](mailto:chenlihua@whut.edu.cn)); Bao-Lian Su ([bao-lian.su@unamur.be](mailto:bao-lian.su@unamur.be))

<sup>a</sup> Laboratory of Living Materials at the State Key Laboratory of Advanced Technology for Materials Synthesis and Processing, Wuhan University of Technology, 122 Luoshi Road, Wuhan, 430070, Hubei, China

<sup>b</sup> International School of Materials Science and Engineering, Wuhan University of Technology, Wuhan, 430070, Hubei, China

<sup>c</sup> Nanostructure Research Center, Wuhan University of Technology, Wuhan, 430070, Hubei, China

<sup>d</sup> School of Chemistry, Chemical Engineering and Life Science, Wuhan University of Technology, Wuhan, 430070, Hubei, China

<sup>e</sup> Laboratory of Inorganic Materials Chemistry, University of Namur, 61 rue de Bruxelles, B-5000 Namur, Belgium

<sup>‡</sup> These authors contributed equally

## Supporting Figures and Tables

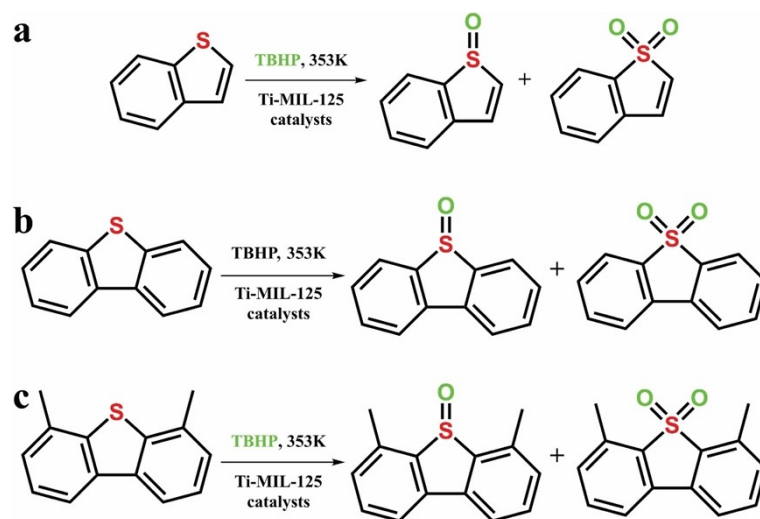


**Figure S1.** Reaction equations of catalytic oxidative desulfurization of (a) BT, (b) DBT, and (c) DMDBT into their oxidative products.

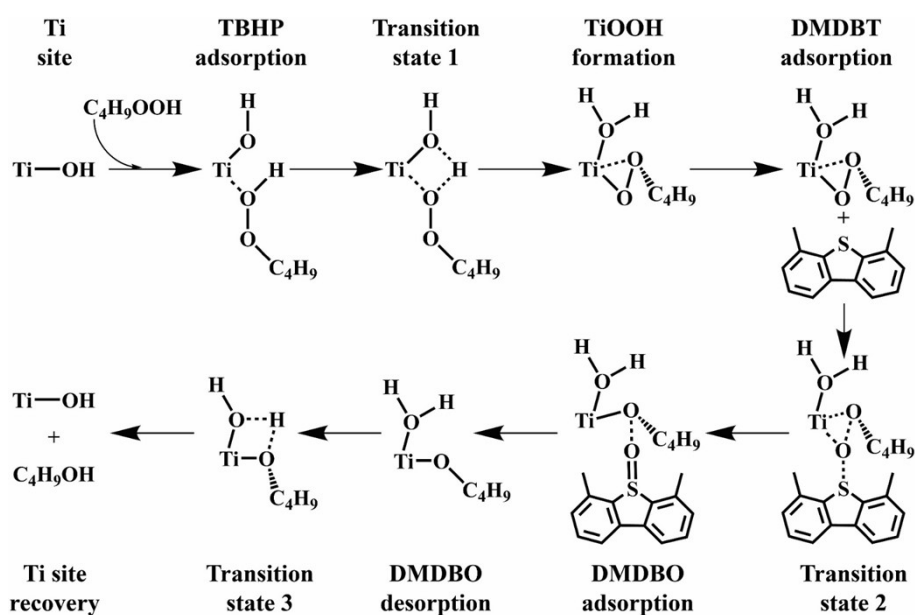


**Figure S2.** Proposed ODS reaction pathway over Ti site of Ti-MIL-125.

Taking the ODS of 4,6-dimethyldibenzothiophene (DMDBT) into 4,6-dimethyldibenzothiophene oxide (DMDBO) for an example (**Figure S2**), **Ti site** adsorbs an oxidation (tert-butyl hydroperoxide, TBHP, C<sub>4</sub>H<sub>9</sub>OOH) to form **TBHP adsorption**, which turns into a transition state (**Transition state 1**) for the formation of reaction intermediate TiOOH (**TiOOH formation**). By adsorption of a reactant DMDBT (**DMDBT adsorption**), it transforms into another transition state (**Transition state 2**) and produce a product DMDBO (**DMDBO adsorption**). After the desorption of DMDBO (**DMDBO desorption**), transition state 3 happens (**Transition state 3**). Finally, Ti site recovers (**Ti site recovery**) after the formation and desorption of product tert-Butanol (TBO).

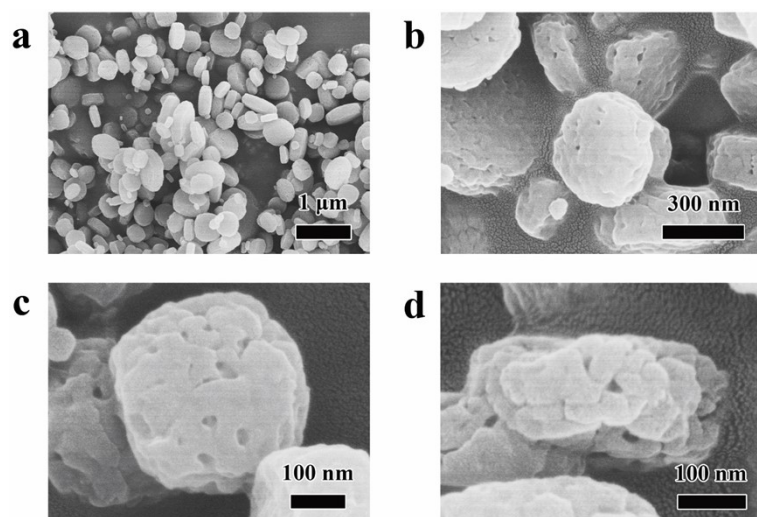


**Figure S3.** SEM images of the Meso-Ti-MIL-125-120C with a crystallization time of 18 h.

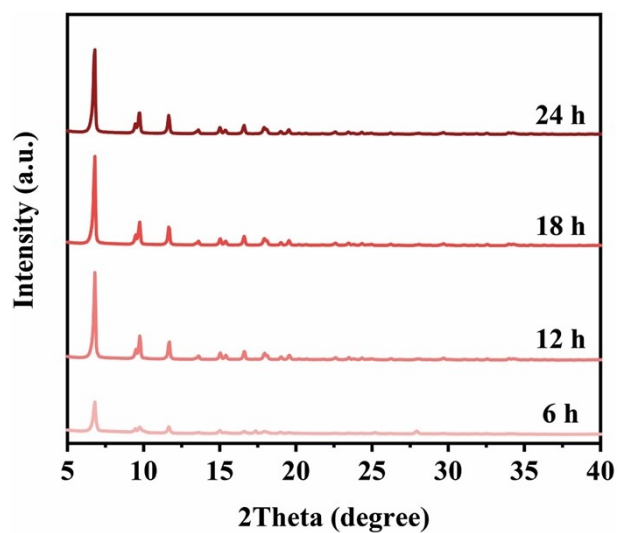


**Figure S4.** XRD patterns of the Meso-Ti-MIL-125-120C obtained with a crystallization time from 6 h to 24 h.

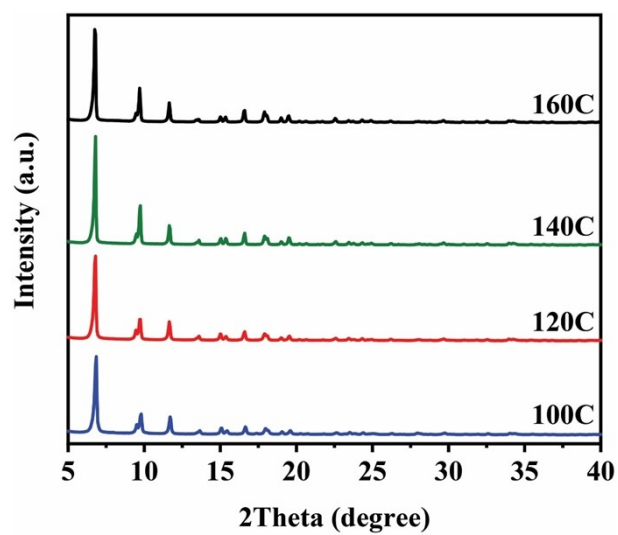


**Figure S5.** XRD patterns of the Meso-Ti-MIL-125 samples obtained under a crystallization temperature from 100°C to 160°C.

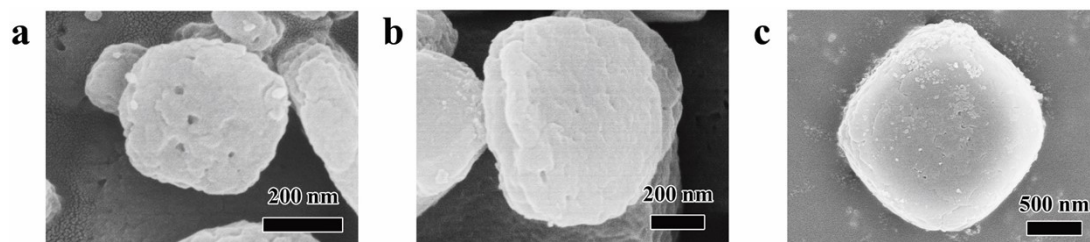


**Figure S6.** SEM images showing the single crystal morphology of the (a) Meso-Ti-MIL-125-100C, (b) Meso-Ti-MIL-125-140C, and (c) Meso-Ti-MIL-125-160C.

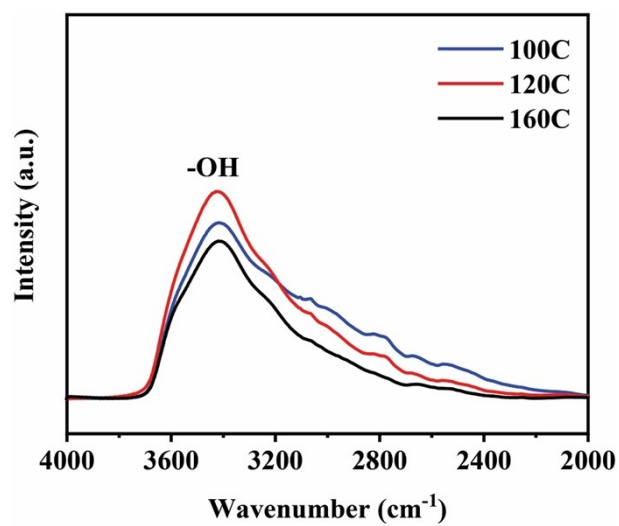


**Figure S7.** FT-IR spectra of the Meso-Ti-MIL-125-100-160C in the range from 4000–2000 cm<sup>-1</sup>.



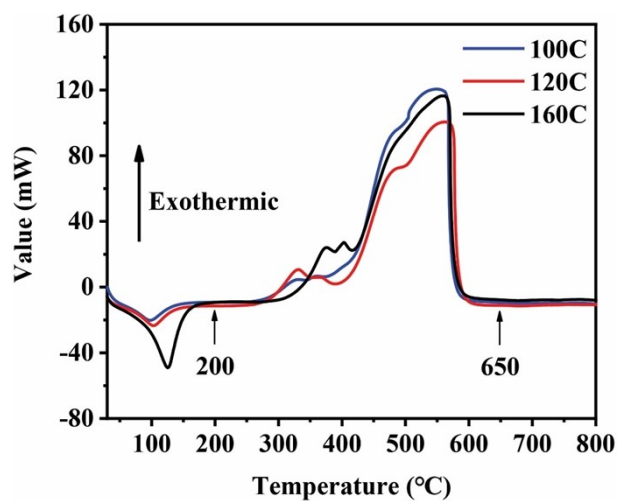


**Figure S8.** DSC curves of the Meso-Ti-MIL-125-100-120C in the air.

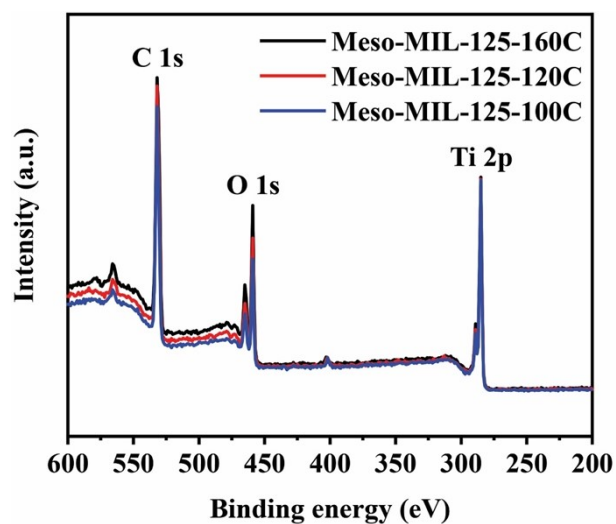


**Figure S9.** XPS results of the Meso-Ti-MIL-125-100–120C showing the signals of C 1s, O 1s, and Ti 2p.

**Table S1.** Textural properties of the Ti-MIL-125 samples

Sample	Surface Ti/O	$S_{BET}$ ( $\text{m}^2\text{g}^{-1}$ )	$S_{micro}$ ( $\text{m}^2\text{g}^{-1}$ )	$S_{exter}$ ( $\text{m}^2\text{g}^{-1}$ )	$V_{tol}$ ( $\text{cm}^3\text{g}^{-1}$ )	$V_{micro}$ ( $\text{cm}^3\text{g}^{-1}$ )	$V_{meso}$ ( $\text{cm}^3\text{g}^{-1}$ )
Meso-MIL-125-100C	0.18	1181	1116	65	0.59	0.47	0.12
Meso-MIL-125-120C	0.20	1401	1325	76	0.71	0.56	0.15
Meso-MIL-125-160C	0.22	1158	1109	49	0.56	0.47	0.09

Surface Ti/O ratio: determined by XPS results,  $S_{BET}$ : BET surface area,  $S_{micro}$ : micropore surface area,  $S_{exter}$ : external surface area,  $V_{total}$ : total pore volume,  $V_{micro}$ : micropore volume,  $V_{meso}$ : mesoporous pore volume obtained by analysis of  $\text{N}_2$  adsorption-desorption data. The micropore and external surface area were determined from  $\text{N}_2$  adsorption using the Brunauer-Emmett-Teller method. Micropore size was calculated by a Horvath-Kawazoe method. Mesopore volume and mesopore size were determined by the desorption branches of  $\text{N}_2$  isotherms, using the Barret-Joyner-Halenda model. Total pore volumes were estimated from the adsorbed amount at a relative pressure  $P/P_0$  of 0.99.

**Table S2.** Catalytic oxidative desulfurization performance of different Meso-MIL-125

catalysts

	BT (%)		DBT (%)		DMDBT (%)	
	1st cycle	5th cycle	1st cycle	5th cycle	1st cycle	5th cycle
<b>Meso-MIL-125-100C</b>	89	\	100	\	73	\
<b>Meso-MIL-125-120C</b>	100	100	100	100	100	100
<b>Meso-MIL-125-160C</b>	42	\	66	\	15	\